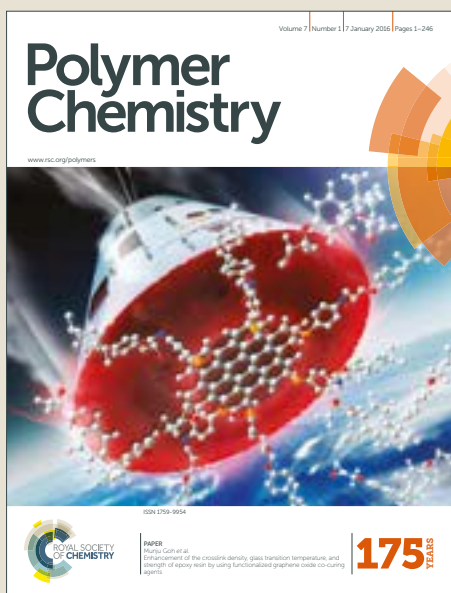


Polymer Chemistry

Accepted Manuscript



This is an Accepted Manuscript, which has been through the Royal Society of Chemistry peer review process and has been accepted for publication.

Accepted Manuscripts are published online shortly after acceptance, before technical editing, formatting and proof reading. Using this free service, authors can make their results available to the community, in citable form, before we publish the edited article. We will replace this Accepted Manuscript with the edited and formatted Advance Article as soon as it is available.

You can find more information about Accepted Manuscripts in the [author guidelines](#).

Please note that technical editing may introduce minor changes to the text and/or graphics, which may alter content. The journal's standard [Terms & Conditions](#) and the ethical guidelines, outlined in our [author and reviewer resource centre](#), still apply. In no event shall the Royal Society of Chemistry be held responsible for any errors or omissions in this Accepted Manuscript or any consequences arising from the use of any information it contains.



Polymer Chemistry

COMMUNICATION

Synthesis of Microcapsules using Inverse Emulsion Periphery RAFT Polymerization via SPG Membrane Emulsification

Received 00th January 20xx,
Accepted 00th January 20xx

Fumi Ishizuka,^a Rhiannon P. Kuchel,^b Hongxu Lu,^c Martina H. Stenzel^{c,*} and Per B. Zetterlund^{a,*}

DOI: 10.1039/x0xx00000x

www.rsc.org/

Hollow particles have the potential for a broad range of applications, but most specifically drug delivery. However, their synthesis can be tedious, requiring techniques such as high energy input or a sacrificial template. Furthermore, loading the final capsules with drugs, catalysts or any other compound is often associated with a low loading efficiency. In this study, we have explored the use of “Shirasu Porous Glass (SPG)” membrane emulsification to create a wide size range of water droplets stabilized with an amphiphilic block copolymer. Polymeric capsules were subsequently created via inverse emulsion periphery RAFT polymerization (IEPP). By changing the pore size of the SPG membrane (0.2–3 μm), we have succeeded in controlling the polymeric microcapsule size from submicron to tens of microns. In addition to this, the process allowed simultaneous and efficient encapsulation of water-soluble compounds such as proteins.

Polymeric nano/microcapsules have a wide range of applications in a number of fields including; biological medicine, the cosmetic and food industries, as well as water treatment and coatings.^{1–4} A number of encapsulation techniques utilizing hollow particles, liposome and emulsion droplets have been developed for the encapsulation of various materials such as anticancer drugs, enzymes, nucleotides, fragrances and catalysts. Hollow polymeric particles have been studied extensively for biomedical applications due to their capacity for encapsulation of therapeutic agents.^{5, 6} There are a variety of approaches to synthesize nano/microcapsules from emulsion based methods, e.g. involving sacrificial templates,^{7–10} dendrimers,¹¹ phase separation¹² and self-assembly.¹³ Typically, each method has associated advantages

and disadvantages. For instance, the template approach provides greater control over size and morphology, but can be rather tedious as it requires removal of the sacrificial template after shell formation. In addition to this, guest molecules normally need to be encapsulated after the removal of the core template; this is because harsh chemicals such as hydrofluoric acid are required to remove the core material. In other words, it requires at least three steps: (i) shell formation, (ii) template removal and (iii) loading. Guest molecules can be encapsulated within nanocapsules in a one pot process via the self-assembly approach, although it is usually difficult to achieve high encapsulation efficiency.^{14–16} The emulsion-based approaches offer a convenient synthetic route to hollow polymeric particles from nano^{17–23} to micron-scale.^{12, 24–28} Oil-in-water systems are typically exploited for the encapsulation of hydrophobic materials,^{29–31} whereas inverse (water-in-oil) systems are suitable for encapsulation of hydrophilic guest molecules.^{32–34}

However, the previously reported emulsion-based techniques may not be appropriate for encapsulation of sensitive molecules such as proteins. This is because the polymerization reaction is occurring within the droplets containing the guest molecules – this may compromise the integrity of the guest molecules. Oil-in-water systems have been extensively studied, however, the resulting capsules have a hydrophobic core, and can consequently not be used for encapsulation of hydrophilic compounds such as proteins. Encapsulation of water-soluble biomolecules such as proteins and nucleotides has received increasing attention over the past decades.^{35–37} For this reason, it is of interest to develop a versatile synthesis approach for nano/microcapsules with hydrophilic core.

^a Centre for Advanced Macromolecular Design, School of Chemical Engineering, The University of New South Wales, Sydney, NSW, 2052, Australia.

^b Electron Microscope Unit, The University of New South Wales, Sydney, NSW, 2052, Australia.

^c Centre for Advanced Macromolecular Design, School of Chemistry, The University of New South Wales, Sydney, NSW, 2052, Australia.

† Footnotes relating to the title and/or authors should appear here.

Electronic Supplementary Information (ESI) available: [details of any supplementary information available should be included here]. See DOI: 10.1039/x0xx00000x

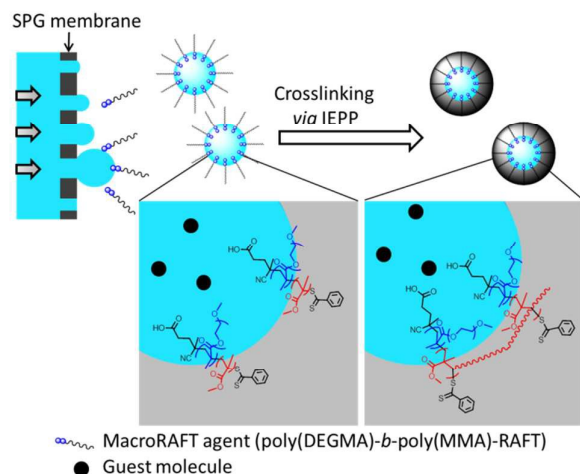


Fig. 1 Schematic illustration of SPG membrane emulsification with macroRAFT stabilizer. The dispersed phase (blue) contains lipophobe and guest molecules, and is passed through pores into the continuous phase by pressure. Crosslinked polymeric shells are formed on the outer surface of the droplets via IEPP.

We have recently pioneered a facile synthesis method for polymeric nanocapsules with hydrophilic core via inverse miniemulsion periphery RAFT polymerization (IMEPP) utilizing amphiphilic diblock copolymers as both an emulsion stabilizer and macroRAFT agent.³⁸⁻⁴³ This approach provides a reaction-free core environment for encapsulation of fragile molecules such as proteins, since the polymerization occurs on the periphery of the droplets as opposed inside the droplets. However, to date, the size range of these polymeric nanocapsules has been limited to approx. 50-500 nm because a conventional emulsification method (ultrasonication) has been used to create the initial inverse miniemulsions. In addition, there have been concerns about the use of high energy input in the form of ultrasonication and its effect on fragile molecules such as proteins remain.

The techniques currently available to create hollow spheres with hydrophilic cargo are either limited by size variation, are multi-step procedures or they have a limited loading efficiency. A truly versatile technique would enable the synthesis of any size depending on the application. However, it is difficult to prepare capsules with a wide size range using conventional emulsification techniques such as ultrasonication. Shirasu Porous Glass membranes (SPG), prepared from Shirasu volcanic ashes in Japan, possess narrow pore size distribution and a wide range of pore sizes are available (0.1-20 μm).⁴⁴⁻⁴⁶ Furthermore, SPG membranes have greater mechanical strength and chemical resistance compared to other types of membranes.^{47, 48} SPG membrane emulsification thus represents one of the most promising techniques for the creation of monodisperse droplets using a low energy approach.

In the present work, SPG membrane emulsification has been employed to prepare inverse emulsions comprising water droplets of adjustable size based on the membrane pore size, using an amphiphilic macroRAFT as stabilizer. The emulsion droplets were subsequently crosslinked via inverse emulsion

periphery RAFT polymerization (IEPP) to obtain polymeric microcapsules.

Inverse emulsions were prepared via SPG membrane emulsification using the amphiphilic macroRAFT agent poly(di(ethylene glycol) methyl ether methacrylate)₁₇-*block*-poly(methyl methacrylate)₉₇ (poly(DEGMA)-*b*-poly(MMA)-RAFT) as a steric stabilizer. The inverse emulsions comprised an organic phase of toluene containing 1 or 0.5 wt% macroRAFT agent (poly(DEGMA)-*b*-poly(MMA)-RAFT, which has a HLB of ~ 5) and an aqueous phase containing 4 wt% lipophobe (sodium carbonate for Exp 2 (Table 1) and sodium chloride for all others). The dispersed phase was pushed through the membrane into the continuous phase by applying pressure with nitrogen gas (Fig. 1). SPG membranes with a range of different pore size (0.1, 0.2, 0.8 and 3 μm) were tested. The emulsification conditions and the resulting droplet diameters are summarized in Table 1. It is well established that the minimum pressure required to generate droplets (the critical pressure, P_c) increases with decreasing pore size.⁴⁷ The maximum pressure for the present module is 500 kPa, which was found to be below P_c for the 0.1 μm membrane. The emulsifying pressures were adjusted to 11, 60 and 275 kPa for the pore sizes of 3.0, 0.8 and 0.2 μm , respectively, slightly higher than the P_c values reported by Nakashima *et al.*⁴⁶ The amount of macroRAFT was varied from 0.005 to 1 wt% (relative to toluene) to test the effect on emulsification using a membrane with pore size 0.8 μm . Stable emulsions were obtained for concentrations above 0.05 wt% macroRAFT (Fig. S2, ESI[†]). For the stable emulsions, no phase separation was observed for at least 30 days at room temperature. However, the 0.2 and 3.0 μm membranes required at least 1 wt% macroRAFT to prepare stable emulsions - the use of 0.5 wt% macroRAFT (Exp 1, 5) led to phase separation during

Table 1 Membrane emulsification conditions and droplet sizes

Exp	Pore size (μm)	Pressure (kPa)	MacroRAFT (wt%) ¹	D_h (μm) ²	$D_{\text{microscope}}$ (μm (\pm SD)) ³
1	0.2	275	0.5	phase separation	
2	0.2	275	1.0	0.54	approx. 1 ^{**}
3	0.8	60	0.5	4.58	2.8 \pm 0.53
4 [*]	0.8	60	0.5	4.78	2.6 \pm 0.43
5	3	13	0.5	phase separation	
6	3	11	1.0	4.42	12.2 \pm 3.0

¹Amount of macroRAFT relative to toluene. ²Hydrodynamic volume average diameter measured by DLS/laser diffraction. ³Average diameter measured by optical microscopy. ^{*}0.01 wt% SRB in the dispersed phase. ^{**}Estimated from Fig. 2a.

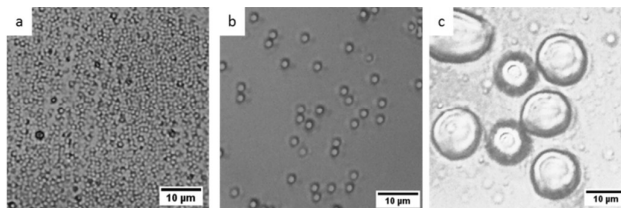


Fig. 2 Optical micrographs of initial droplets prepared by SPG membrane with pore size of 0.2 (a), 0.8 (b) and 3.0 μm (c).

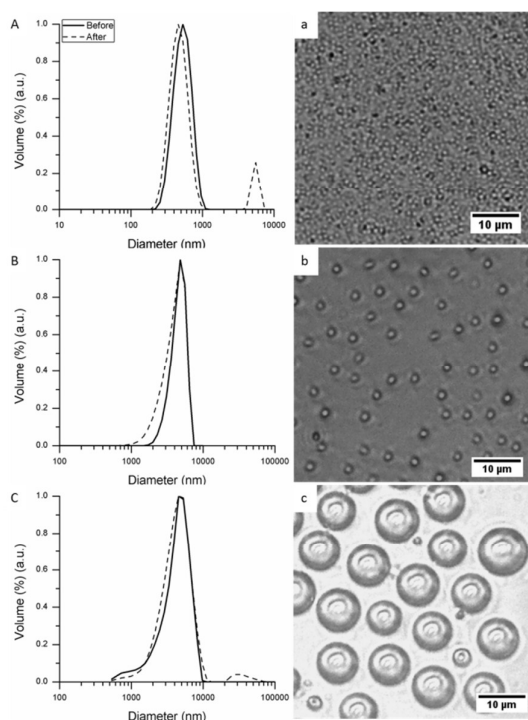


Fig. 3 Droplet/particle size distribution by volume of before (solid line) and after polymerization (dashed line); (A) Exp. 2 (0.2 μm), (B) Exp. 3 (0.8 μm), (C) Exp. 6 (3.0 μm) and optical micrographs of crosslinked microcapsules. Membrane pore size: 0.2 (a), 0.8 (b) and 3.0 μm (c)

emulsification. Stable emulsions (Exp 2, 3, 4 and 6) were observed by optical microscopy (Fig. 2). The droplet diameters calculated by graphical analysis are summarized in Table 1 (for Exp 2, the diameter was too small for such analysis). The droplet diameters increased with increasing pore size (Fig. 2), and exhibited relatively narrow distributions (Fig. 2). The droplet diameters were approximately 3-4 times larger than the pore size, in good agreement with previous reports.^{47, 48} The hydrodynamic diameters were also measured by light scattering (DLS for Exp 2, 3, 4 and laser diffraction for Exp 6 (Table 1, Fig. 3A-C)), revealing monomodal distributions in all cases (Fig. 3A-C, Table 1, S3 and S4 in ESI[†]). The results support our findings with regard to diameter size observed by optical microscopy for Exp 2, 3 and 4, while the volume mean diameter of Exp 6 was smaller than the diameter confirmed by optical micrography. This discrepancy may be caused by the presence of smaller droplets (Exp 6) not detected by the graphical analysis software (Fig. 2c). We also observed the initial inverse emulsion (Exp 3) by cryoTEM (Fig. S6, ESI[†]). The droplet diameter was approximately 3 μm , concurrent with our observations using optical micrography. Interestingly, the droplets appeared hexagonal presumably due to the high concentration. It is believed that the amphiphilic copolymer forms a thin flexible layer around the water droplets and thus prevents the droplets from merging. When monodisperse spherical particles are packed tightly, they are known to form a hexagonal shape.⁴⁹

To create polymeric shells around the water droplets, inverse emulsion periphery RAFT polymerization was carried

out after emulsification. According to the IMEPP procedure,³⁸⁻⁴³ the water droplets act as templates, thereby directing the growth of crosslinked polymeric shells forming via the RAFT mechanism around the periphery of the droplets. The crosslinking RAFT polymerization was conducted using the monomers MMA and EGDMA (dissolved in the toluene continuous phase) at 60 $^{\circ}\text{C}$ using AIBN as initiator (recipe in Table S2, ESI).

In all cases, the polymerizations were carried out successfully leading to crosslinked polymeric microcapsules. The total conversion of MMA and EGDMA were 15, 34, 12 and 15% after 6 h for Exp 2, 3, 4 and 6, respectively. Optical micrographs (Fig. 3a-c) revealed microcapsules comprising very thin shells with somewhat smaller diameter compared to the initial droplets, but with relatively narrow size distributions. Transmission electron micrographs also confirmed the presence of polymeric capsules (Fig. 4). The thickness of the polymeric shells was approximately 20-60 nm for all polymerizations. The microcapsules appear somewhat larger in the TEM images than in the optical micrographs. In an optical microscope, samples are observed in the liquid state whilst TEM imaging involves dessication of the sample, possibly leading to a flattened morphology. The size of the microcapsules was also measured by light scattering after polymerization. The main peaks shifted slightly to smaller diameters (Fig. 3A-C, Table S3 and S4). The decrease in diameter and the secondary peaks in Fig. 3A and 3C may be due to emulsion degradation (no significant inter-particle crosslinking was observed by optical microscopy). As mentioned previously, the emulsions were stable at room temperature for at least one month (Fig S3, ESI[†]). However, when heated at 60 $^{\circ}\text{C}$ (the polymerization temperature), degradation was observed to some extent (Fig S4 and S5, ESI[†]).

To investigate whether the encapsulation of guest molecules would affect the microcapsule synthesis, a water-soluble fluorescent dye (Sulforhodamine B, SRB) was incorporated in the dispersed phase. Encapsulation of this water-soluble dye did not have any significant effect on the droplet/microcapsule diameter (Table 1). Fig. 5 shows

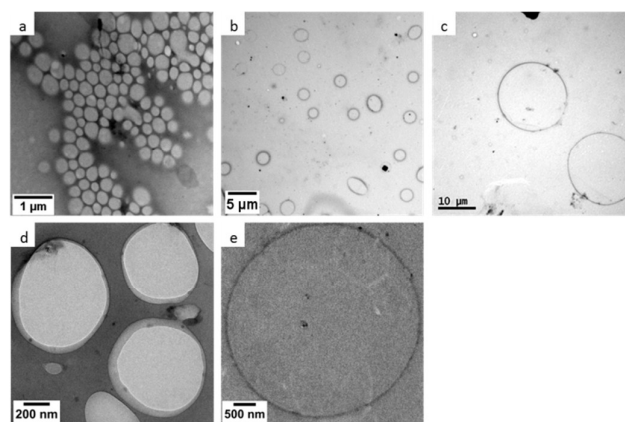


Fig. 4 TEM micrographs of crosslinked microcapsules. Membrane pore size : 0.2 (a, d), 0.8 (b, e) and 3.0 μm (c).

microcapsules after polymerization (Exp 4) encapsulating SRB as a fluorescent model compound. The red regions, corresponding to the aqueous interior of the capsules, are similar in size to the optical micrograph estimate (Table 1). The presence of guest molecules did not affect the size, and encapsulation was successfully achieved with high efficiency (~97% according to fluorescence spectroscopy).

Fluorescein-labelled bovine serum albumin (FBSA) was also used as a model compound and successfully encapsulated within microcapsules without significant effect on microcapsule size (0.8 and 3 μm membranes, same conditions as Exp 3 and 6; Fig. 5b and S7, ESI[†]). This demonstrates that not only small molecules but also proteins can be trapped in the aqueous domain of the capsule at quantitative encapsulation efficiencies (Table S5, ESI[†]). This simple IEPP process can be employed for encapsulation of various water-soluble guest molecules such as gemcitabine in polymeric capsules at high efficiency.⁴¹ Polymeric capsules can be prepared by a number of established approaches; however, the encapsulation of hydrophilic materials at high efficiency (over 90%) remains challenging.^{50, 51} Compared to synthetic approaches such as coacervation and spray drying,^{52, 53} the IEPP process offers a facile route to encapsulation of water-soluble molecules including anti-cancer drugs and proteins in a wide size range of capsules (nano to micro scale). Due to the insolubility of proteins in the organic media, the encapsulation efficiency for large charged molecules in this process is close to 100%. It is also worth mentioning that our previous study showed the capsules to be non-toxic after post purification and functionalization.⁴¹

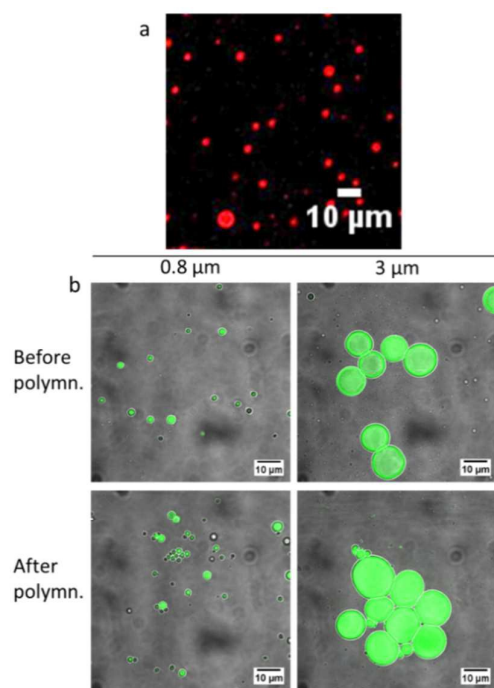


Fig. 5 Laser scanning confocal micrographs of microcapsules containing SRB (a), FBSA (b). Scale bars, 10 μm .

Conclusions

Polymeric microcapsules with a hydrophilic core were successfully synthesized using SPG membrane emulsification in tandem with the IEPP technique. Inverse emulsions with a relatively narrow size distribution were prepared using an amphiphilic macroRAFT comprising poly(di(ethylene glycol) methyl ether methacrylate) and poly(methyl methacrylate). By changing the SPG membrane pore size (0.2 to 3.0 μm), we have managed to successfully control the droplet size from 0.5 (with 0.2 μm membrane) - 12 μm (with 3 μm membrane), and subsequently the size of the final capsules. This broad size range cannot be achieved by conventional emulsion based techniques such as (mini)emulsion or suspension system, which typically produce either much smaller or larger particles. These synthesized emulsions exhibit high stability at room temperature and maintain their size and size distribution after polymerization. We have also demonstrated the facile encapsulation of water-soluble dye which could be easily replaced with other water soluble compounds such as drugs. Overall, the IEPP process can be applied to a wide size range of droplets, enabling the encapsulation of various molecules in nano/microcapsules.

Notes and references

- 1 A. C. Hunter, J. Elsom, P. P. Wibroe and S. M. Moghimi, *Maturitas*, 2012, **73**, 5-18.
- 2 Z. Xiao, W. Liu, G. Zhu, R. Zhou and Y. Niu, *J. Sci. Food Agric.*, 2014, **94**, 1482-1494.
- 3 D. Setyono and S. Valiyaveetil, *RSC Adv.*, 2015, **5**, 83286-83294.
- 4 M. Samadzadeh, S. H. Boura, M. Peikari, S. M. Kasirha and A. Ashrafi, *Prog. Org. Coat.*, 2010, **68**, 159-164.
- 5 G.-D. Fu, G. L. Li, K. G. Neoh and E. T. Kang, *Prog. Polym. Sci.*, 2011, **36**, 127-167.
- 6 L. A. Frank, R. V. Contri, R. C. Beck, A. R. Pohlmann and S. S. Guterres, *Wiley Interdiscip. Rev.: Nanomed. Nanobiotechnol.*, 2015, **7**, 623-639.
- 7 C. Boyer, M. R. Whittaker, C. Nouvel and T. P. Davis, *Macromolecules*, 2010, **43**, 1792-1799.
- 8 X. Liu and A. Basu, *J. Am. Chem. Soc.*, 2009, **131**, 5718-5719.
- 9 S. R. S. Ting, A. M. Gregory and M. H. Stenzel, *Biomacromolecules*, 2009, **10**, 342-352.
- 10 B. Huang, S. Zhou, M. Chen and L. Wu, *Macromolecules*, 2014, **47**, 1914-1921.
- 11 A. Sunder, M. Kramer, R. Hanselmann, R. Mulhaupt and H. Frey, *Angew. Chem. Int. Ed.*, 1999, **38**, 3552-3555.
- 12 W. F. Gu, S. R. S. Ting and M. H. Stenzel, *Polymer*, 2013, **54**, 1010-1017.
- 13 D. Kim, E. Kim, J. Lee, S. Hong, W. Sung, N. Lim, C. G. Park and K. Kim, *J. Am. Chem. Soc.*, 2010, **132**, 9908-9919.
- 14 C. Zhou, M. Wang, K. Zou, J. Chen, Y. Zhu and J. Du, *ACS Macro Letters*, 2013, **2**, 1021-1025.
- 15 I. K. Jeong, G. H. Gao, Y. Li, S. W. Kang and D. S. Lee, *Macromol. Biosci.*, 2013, **13**, 946-953.
- 16 I. Hofmeister, K. Landfester and A. Taden, *Angew. Chem. Int. Ed.*, 2015, **54**, 327-330.
- 17 P. B. Zetterlund, Y. Saka and M. Okubo, *Macromol. Chem. Phys.*, 2008, **210**, 140-149.

- 18 W. Li, K. Matyjaszewski, K. Albrecht and M. Möller, *Macromolecules*, 2009, **42**, 8228-8233.
- 19 W. Li, J. A. Yoon and K. Matyjaszewski, *J. Am. Chem. Soc.*, 2010, **132**, 7823-7825.
- 20 A. J. P. van Zyl, R. F. P. Bosch, J. B. McLeary, R. D. Sanderson and B. Klumperman, *Polymer*, 2005, **46**, 3607-3615.
- 21 Y. Luo and H. Gu, *Polymer*, 2007, **48**, 3262-3272.
- 22 K. Ohno, Y. Ma, Y. Huang, C. Mori, Y. Yahata, Y. Tsujii, T. Maschmeyer, J. Moraes and S. Perrier, *Macromolecules*, 2011, **44**, 8944-8953.
- 23 K. Landfester, *Angew. Chem. Int. Ed.*, 2009, **48**, 4488-4507.
- 24 M. Ito, Y. Furukawa, H. Minami and M. Okubo, *Colloid. Polym. Sci.*, 2008, **286**, 1335-1341.
- 25 Y. Konishi, M. Okubo and H. Minami, *Colloid. Polym. Sci.*, 2003, **281**, 123-129.
- 26 M. Okubo, Y. Konishi, T. Inohara and H. Minami, *Colloid. Polym. Sci.*, 2003, **281**, 302-307.
- 27 M. Okubo, Y. Konishi and H. Minami, *Prog. Colloid Polym. Sci.*, 2004, **124**, 54-59.
- 28 M. Okubo, Y. Konishi and H. Minami, *Colloid. Polym. Sci.*, 2001, **279**, 519-523.
- 29 H. Minami, H. Fukaumi, M. Okubo and T. Suzuki, *Colloid. Polym. Sci.*, 2012, **291**, 45-51.
- 30 H. Minami, M. Okubo and Y. Oshima, *Polymer*, 2005, **46**, 1051-1056.
- 31 P. Chaiyasat, Y. Ogino, T. Suzuki and M. Okubo, *Colloid. Polym. Sci.*, 2008, **286**, 753-759.
- 32 F. Lu, Y. Luo, B. Li, Q. Zhao and F. J. Schork, *Macromolecules*, 2010, **43**, 568-571.
- 33 Y. Wang, G. Jiang, M. Zhang, L. Wang, R. Wang and X. Sun, *Soft Matter*, 2011, **7**, 5348-5352.
- 34 E.-M. Rosenbauer, K. Landfester and A. Musyanovych, *Langmuir*, 2009, **25**, 12084-12091.
- 35 R. Jalil and J. R. Nixon, *J. Microencapsulation*, 1990, **7**, 297-325.
- 36 L. J. De Cock, S. De Koker, B. G. De Geest, J. Grooten, C. Vervaet, J. P. Remon, G. B. Sukhorukov and M. N. Antipina, *Angew. Chem. Int. Ed.*, 2010, **49**, 6954-6973.
- 37 A. W. Du and M. H. Stenzel, *Biomacromolecules*, 2014, **15**, 1097-1114.
- 38 R. H. Utama, M. Drechsler, S. Förster, P. B. Zetterlund and M. H. Stenzel, *ACS Macro Letters*, 2014, **3**, 935-939.
- 39 R. H. Utama, M. Dulle, S. Forster, M. H. Stenzel and P. B. Zetterlund, *Macromol. Rapid Commun.*, 2015, **36**, 1267-1271.
- 40 R. H. Utama, Y. Guo, P. B. Zetterlund and M. H. Stenzel, *Chem. Commun.*, 2012, **48**, 11103-11105.
- 41 R. H. Utama, Y. Jiang, P. B. Zetterlund and M. H. Stenzel, *Biomacromolecules*, 2015, **16**, 2144-2156.
- 42 R. H. Utama, M. H. Stenzel and P. B. Zetterlund, *Macromolecules*, 2013, **46**, 2118-2127.
- 43 F. Ishizuka, R. H. Utama, S. Kim, M. H. Stenzel and P. B. Zetterlund, *Eur. Polym. J.*, 2015, **73**, 324-334.
- 44 K. Kandori, K. Kishi and T. Ishikawa, *Colloids Surf.*, 1991, **55**, 73-78.
- 45 K. Kandori, K. Kishi and T. Ishikawa, *Colloids Surf.*, 1991, **61**, 269-279.
- 46 T. Nakashima, M. Shimizu and M. Kukizaki, *Key Eng. Mater.*, 1991, **61-62**, 513-516.
- 47 S. M. Joscelyne and G. Trägårdh, *J. Membr. Sci.*, 2000, **169**, 107-117.
- 48 C.-J. Cheng, L.-Y. Chu and R. Xie, *J. Colloid Interface Sci.*, 2006, **300**, 375-382.
- 49 M. A. Winnik, *Curr. Opin. Colloid Interface Sci.*, 1997, **2**, 192-199.
- 50 V. J. Mohanraj, T. J. Barnes and C. A. Prestidge, *Int. J. Pharm.*, 2010, **392**, 285-293.
- 51 S. Vicente, M. Peleteiro, B. Díaz-Freitas, A. Sanchez, Á. González-Fernández and M. J. Alonso, *J. Control. Release*, 2013, **172**, 773-781.
- 52 J. Wu, Q. Fan, Y. Xia and G. Ma, *Chem. Eng. Sci.*, 2015, **125**, 85-97.
- 53 P. L. Lam and R. Gambari, *J. Control. Release*, 2014, **178**, 25-45.

